

Synthesis, characterization, and morphological control of $\text{Na}_{1/2}\text{Bi}_{1/2}\text{Cu}_3\text{Ti}_4\text{O}_{12}$ through modify sol–gel method

Majid Ramezani¹ · Ali Sobhani-Nasab² · S. Mostafa Hosseinpour-Mashkani²

Received: 31 January 2015 / Accepted: 21 March 2015 / Published online: 28 March 2015
© Springer Science+Business Media New York 2015

Abstract This paper describes the synthesis of $\text{Na}_{1/2}\text{Bi}_{1/2}\text{Cu}_3\text{Ti}_4\text{O}_{12}$ (BNCTO) with different morphologies like nanoparticles, micro cubic, and micro sheet structure prepared by modify sol–gel method, using different surfactants (SDS, CTAB, PVP, and PVA). This study aimed to investigate the effects of different surfactant such as SDS, CTAB, PVP, and PVA and chelating agent on the morphology and particle size of final products. It was found that the size and morphology of the products could be greatly influenced by the aforementioned parameters. To our knowledge, this is the first report on the synthesis of $\text{Na}_{1/2}\text{Bi}_{1/2}\text{Cu}_3\text{Ti}_4\text{O}_{12}$ nanostructure with different morphologies in the presence of salicylic acid as a chelating agent. The as-synthesized products were characterized by powder X-ray diffraction, scanning electronic microscopy, ultraviolet–visible, and energy dispersive spectrometry analysis of X-ray techniques.

1 Introduction

In recent years, there has been considerable interest in nanocrystalline materials, due to increase activity and a large surface-to-volume ratio and special optical, electrical, and magnetic properties as compared to those of the bulk

materials [1–4]. Recently, many perovskite-like oxides $\text{ACu}_3\text{Ti}_4\text{O}_{12}$ nanostructures ($A = \text{Ca}, \text{La}_{2/3}, \text{Bi}_{1/2}\text{Na}_{1/2}$, etc.) with body-centered cubic crystal structure, have drawn considerable theoretical and experimental studies [5–9]. There is considerable interest in a family of isostructural compounds $\text{ACu}_3\text{Ti}_4\text{O}_{12}$, where $A = \text{Ca}, \text{La}_{2/3}, \text{Na}_{1/2}\text{Y}_{1/2}$, etc. [10–18]. All possess a perovskite-related crystal structure where the TiO_6 octahedra are sufficiently in-phase tilted to produce a square planar environment for Cu. To date, all of these phases are cubic and centric space group $Im-3$, at least at room temperature. $\text{CaCu}_3\text{Ti}_4\text{O}_{12}$ (CCTO) is the most studied compound from this family since fixed (radio) frequency measurements on single crystals [12], and ceramics [10, 11, 13–18], show a “so-called” giant permittivity (>1000) over a wide temperature range, ~ 150 – 400 K. There has been much speculation on the origin of the giant permittivity, especially for single crystals; however, a combination of impedance spectroscopy [13], microcontact measurements across single grain boundaries [14], and Kelvin probe microscopy [14], has shown CCTO ceramics to be electrically heterogeneous with semiconducting grains and insulating grain boundaries. Such an electrical microstructure is consistent with an internal barrier layer capacitor; the “giant” permittivity observed from fixed frequency measurements is an extrinsic effect associated with thin insulating grain boundaries. Low temperature impedance spectroscopy and fixed frequency measurements show the bulk permittivity of CCTO to be ~ 100 . We report here the synthesis and characterization of $\text{Na}_{1/2}\text{Bi}_{1/2}\text{Cu}_3\text{Ti}_4\text{O}_{12}$ (BNCTO) through the modify sol–gel method. Besides, several experiments were performed in order to investigate the effect of surfactants such as SDS, CTAB, PVP, and PVA, and chelating agent (salicylic acid) on the morphology and particle size of final products.

✉ S. Mostafa Hosseinpour-Mashkani
Hosseinpour.sm@gmail.com

¹ Department of Chemistry, Arak Branch, Islamic Azad University, Arak, Iran

² Young Researchers and Elites Club, Arak Branch, Islamic Azad University, Arak, Iran

2 Experimental

2.1 Characterization

X-ray diffraction (XRD) patterns were recorded by a Philips-X'PertPro, X-ray diffractometer using Ni-filtered Cu $K\alpha$ radiation at scan range of $10 < 2\theta < 80$. Scanning electron microscopy (SEM) images were obtained on LEO-1455VP equipped with an energy dispersive X-ray spectroscopy. Fourier transform infrared (FT-IR) spectrum was recorded on a magna Nicolet 550 spectrophotometer in KBr pellets. The energy dispersive spectrometry (EDS) analysis was studied by XL30, Philips microscope. The diffused reflectance UV–visible spectrum (DRS) of the sample was recorded by an Ava Spec-2048TEC spectrometer.

2.2 Synthesis of $\text{Na}_{1/2}\text{Bi}_{1/2}\text{Cu}_3\text{Ti}_4\text{O}_{12}$ nanostructure

The bismuth nitrate ($\text{Bi}(\text{NO}_3)_3 \cdot 5\text{H}_2\text{O}$), copper (II) acetate ($\text{Cu}(\text{CH}_3\text{COO})_2$), sodium nitrate (NaNO_3), and titanium tetraisopropoxide (TTIP) were purchased from Merck Company and used without further purification. In a typical synthesis, the stoichiometric amount of $\text{Bi}(\text{NO}_3)_3 \cdot 5\text{H}_2\text{O}$ (1 mmol), NaNO_3 (1 mmol), $\text{Cu}(\text{CH}_3\text{COO})_2$ (6 mmol), NaNO_3 , and TTIP (8 mmol) were dissolved in 20 ml ethanol under stirring to form a homogeneous solution. Afterwards, salicylic acid (24 mmol) as chelating agent and SDS (4 mmol) as surfactant were separately dissolved in ethanol and added to the above solution under constant stirring. Subsequently, the final mixed solution was kept stirring to form a gel at 60 °C. Finally, the obtained product was calcinated at 600 and 900 °C for 5 and 3 h in a conventional furnace in air atmosphere, respectively. The as-synthesized powders were characterized by SEM, XRD, and EDS. The synthesis conditions of $\text{Na}_{1/2}\text{Bi}_{1/2}\text{Cu}_3\text{Ti}_4\text{O}_{12}$ (BNCTO) nanostructure are listed in Table 1.

3 Results and discussion

The XRD patterns of pure $\text{Na}_{1/2}\text{Bi}_{1/2}\text{Cu}_3\text{Ti}_4\text{O}_{12}$ (BNCTO) in the presence of PVA as surfactant and salicylic acid as chelating agent (sample 1) and sample 5 are shown in

Fig. 1a, b. Extremely broaden reflection peaks were observed in Fig. 1a, b, which indicated fine particle nature of the obtained orthorhombic phase of BNCTO nanostructures with space group of $Fmmm$ (JCPDS card No. 46-0725). No other crystalline phases were detected in the calcined product. In XRD pattern of sample 1, peaks can be indexed as (006), (001), (117), (200), (206), (001), (006), (228), (221), (311), and (335) diffraction lines. From XRD data, the crystallite diameter (D_c) of BNCTO nanostructures obtained from sample 1 was calculated to be 32 nm using the Scherer equation [19]:

$$D_c = K\lambda / \beta \cos\theta \quad \text{Scherer equation}$$

where β is the breadth of the observed diffraction line at its half intensity maximum (117), K is the so-called shape factor, which usually takes a value of about 0.9, and λ is the wavelength of X-ray source used in XRD. Chemical composition and purity of the as-synthesized BNCTO nanostructures was investigated by EDS analysis. The EDS spectrum of BNCTO obtained from sample 1 is shown in Fig. 2. According to the Fig. 2, Ti, O, Cu, Ni, and Bi elements are observed in the EDS spectrum. In addition, neither N nor C signals were detected in the EDS spectrum, which means the product is pure and free of any surfactant or impurity. The diffused reflectance spectrum of the as-prepared BNCTO nanostructures (sample 1) is shown in Fig. 3. The fundamental absorption edge in most semiconductors follows the exponential law. Using the absorption data the band gap was estimated by Tauc's relationship:

$$\alpha = \alpha_0 (h\nu - E_g)^n / h\nu$$

where α is absorption coefficient, $h\nu$ is the photon energy, α_0 and h are the constants, E_g is the optical band gap of the material, and n depends on the type of electronic transition and can be any value between 1/2 and 3 [4]. The E_g values is calculated as 4.47 eV for the BNCTO (sample 1). FT-IR analysis was carried out to identify the presence of certain functional groups in the BNCTO nanostructures and confirm the purity of BNCTO; therefore, the FT-IR spectrum of BNCTO nanostructures (sample 1) was recorded in the range of 400–4000 cm^{-1} (Fig. 4). According to the Fig. 4,

Table 1 Reaction conditions for $\text{Na}_{1/2}\text{Bi}_{1/2}\text{Cu}_3\text{Ti}_4\text{O}_{12}$ nanostructure

Sample no.	Solvent	Chelating agent	Surfactant	Morphology
1	Ethanol	Salicylic acid	PVA	Nanoparticles
2	Ethanol	Salicylic acid	CTAB	Cubic microstructure
3	Ethanol	Salicylic acid	SDS	Cubic microstructure
4	Ethanol	Salicylic acid	PVP	Microstructures
5	Ethanol	–	PVA	Micro sheet
6	Ethanol	–	CTAB	Microstructures
7	Ethanol	–	SDS	Cubic microstructure
8	Ethanol	–	PVP	Microstructure

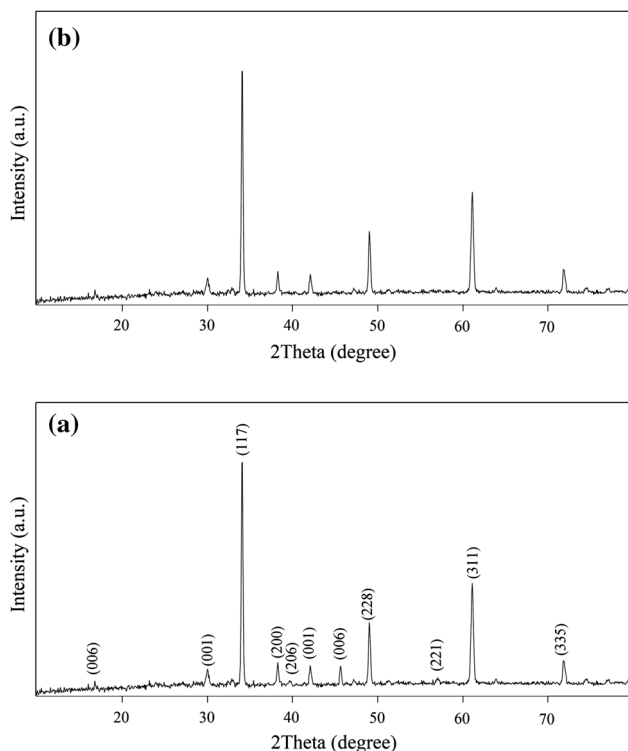


Fig. 1 XRD patterns of $\text{Na}_{1/2}\text{Bi}_{1/2}\text{Cu}_3\text{Ti}_4\text{O}_{12}$ nanostructure. **a** Sample 1, **b** sample 5

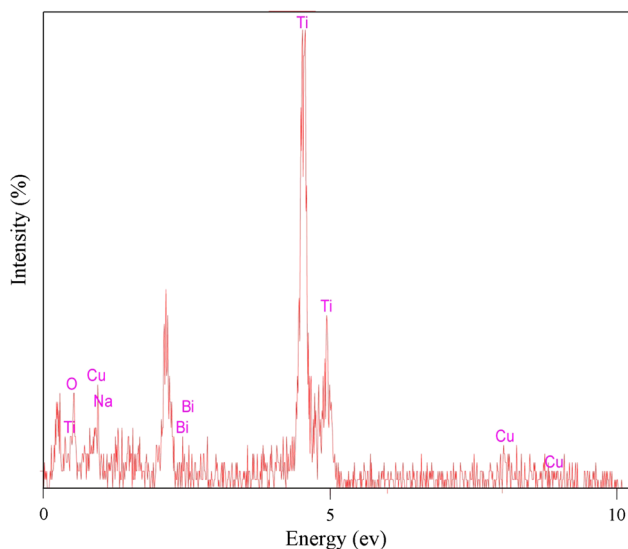


Fig. 2 EDS pattern of $\text{Na}_{1/2}\text{Bi}_{1/2}\text{Cu}_3\text{Ti}_4\text{O}_{12}$ nanostructure (sample 1)

absorption bands at 3423 and 1623 cm^{-1} are attributable to the $\nu(\text{OH})$ stretching and bending vibrations, respectively, which indicates the presence of physisorbed water molecules linked to BNCTO nanostructure [20]. Furthermore, the strong absorptions bond at 620 cm^{-1} is attributed to the stretching of Ti–O. The sharp absorption band appearing at 1114 cm^{-1} can be assigned to the C–O group [21]. In

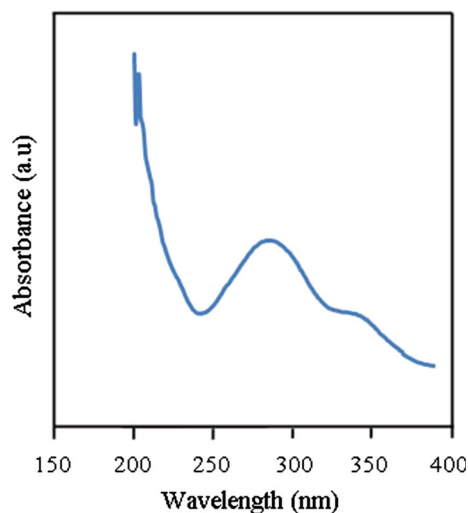


Fig. 3 Diffuse reflectance spectrum of $\text{Na}_{1/2}\text{Bi}_{1/2}\text{Cu}_3\text{Ti}_4\text{O}_{12}$ nanostructure (sample 1)

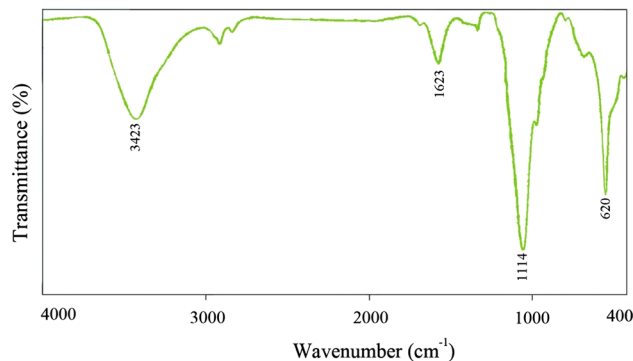


Fig. 4 FT-IR spectrum of $\text{Na}_{1/2}\text{Bi}_{1/2}\text{Cu}_3\text{Ti}_4\text{O}_{12}$ nanostructure (sample 1)

recent years, there has been considerable interest in control the shape and particle size of nanostructures through the control reaction parameters thanks to the fact that properties of nanostructures are highly depend on their particle size and shape; therefore, we performed several experiments to investigate the effect of surfactants such as SDS, CTAB, PVP, and PVA and chelating agent on the morphology and particle size of the $\text{Na}_{1/2}\text{Bi}_{1/2}\text{Cu}_3\text{Ti}_4\text{O}_{12}$ (BNCTO) nanostructures. Figure 5a–d show the SEM images of BNCTO in the presence of salicylic acid as a chelating agent and PVP, CTAB, SDS, and PVA as surfactants accordance with sample 1–4, respectively. Based on the Fig. 5a, product mainly consists of homogenous nanoparticles with average diameter size between ~ 15 – 25 nm . By changing surfactant from PVP to CTAB and SDS morphology of final products were changed to the cubic microstructure; however, use SDS as surfactant causes decrease in the size of cubic structure, as shown in Fig. 5b, c, respectively. In the presence of PVA (sample 4,

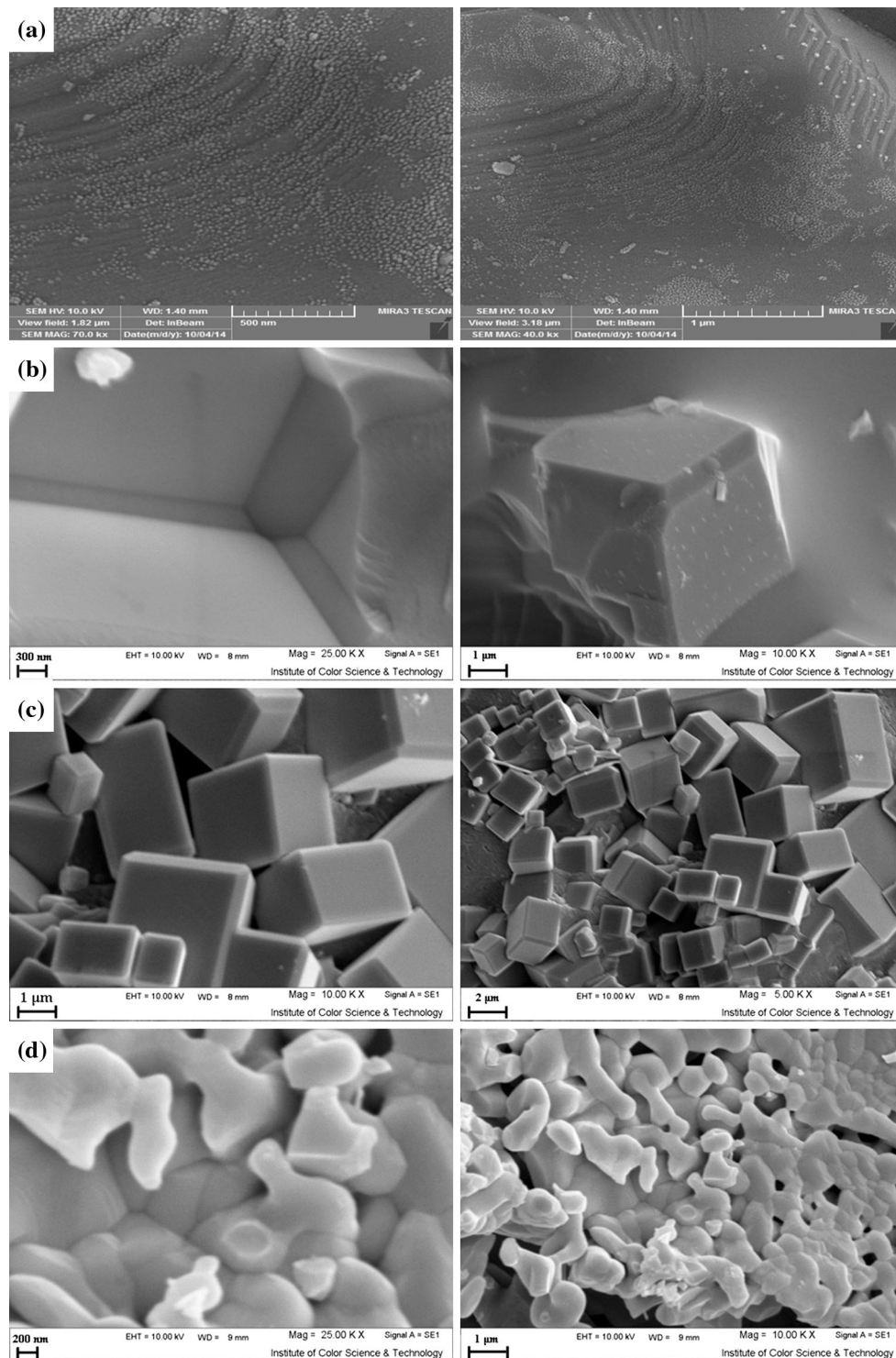


Fig. 5 SEM images of $\text{Na}_{1/2}\text{Bi}_{1/2}\text{Cu}_3\text{Ti}_4\text{O}_{12}$ nanostructure. **a** Sample 1, **b** sample 2, **c** sample 3, **d** sample 4

Fig. 5d) product consists of microstructures. To investigate the effect of salicylic acid as a chelating agent four experiments were performed without salicylic acid in the presence of same surfactants PVP, CTAB, SDS, and PVA accordance with sample 5–8 (Fig. 6a–d), respectively. In

the absence of chelating agent with same surfactant (PVP) morphology of BNCTO was change from homogenous nanoparticles (sample 1) to micro sheet structure (sample 5), as shown in Fig. 6a. It can be observed from SEM image of sample 6 that product consists of microstructures

(Fig. 6b). By applying SDS as surfactant (sample 7) in the absence of chelating agent, morphology of products is cubic microstructure, as shown in Fig. 6c. Based on the Fig. 6d, products consist of micro structure in the present of PVP (sample 8) as surfactant and in the absence of

salicylic acid as a chelating agent. In comparison samples in the presence of chelating agent (sample 1–4) with samples in the absence of chelating agent (sample 5–8), applying salicylic acid as a chelating agent causes decrease in the size of final product.

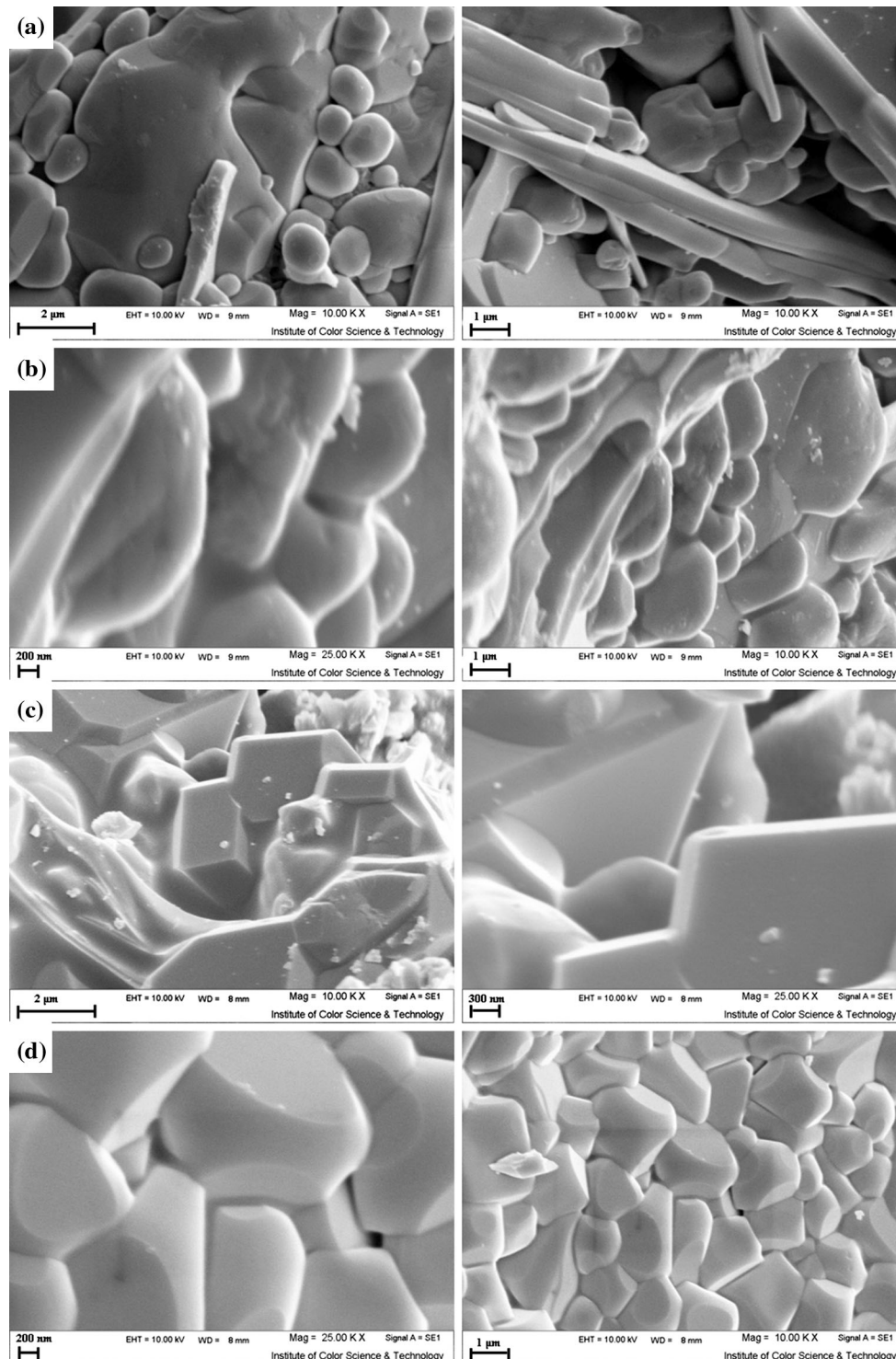


Fig. 6 SEM images of $\text{Na}_{1/2}\text{Bi}_{1/2}\text{Cu}_3\text{Ti}_4\text{O}_{12}$ nanostructure. **a** Sample 5, **b** sample 6, **c** sample 7, **d** sample 8

4 Conclusions

In this route, we applied various surfactants and obtained $\text{Na}_{1/2}\text{Bi}_{1/2}\text{Cu}_3\text{Ti}_4\text{O}_{12}$ (BNCTO) nanostructures with different morphology through modify sol–gel method in the presence and absence chelating agent. The experimental results reveal that the type of surfactant and presence and absence of chelating agent play an important role in the morphology control of the final products. It is first report that shape control of BNCTO nanostructures can be achieved by changing the surfactant and chelating agent and nanoparticles, micro cubic, and micro sheet structure of BNCTO were successfully synthesized. Furthermore, it is the first time that salicylic acid was used as chelating agent for the synthesis of BNCTO nanostructures.

Acknowledgments Authors are grateful to council of University of Arak for providing financial support to undertake this work.

References

1. H. Zeynali, H. Akbari, R.K. Ghasabeh, Y. Azizian-Kalandaragh, S.M. Hosseinpour-Mashkani, *J. Supercond. Nov. Magn.* **26**, 713 (2012)
2. R. Dittmer, E.M. Anton, W. Jo, H. Simons, J.E. Daniels, M. Hoffman, J. Pokorny, I.M. Reaney, J. Rodel, *J. Am. Ceram. Soc.* **1–6**, 3519 (2012)
3. H. Zeynali, S.B. Mousavi, S.M. Hosseinpour-Mashkani, *Mater. Lett.* **144**, 65 (2015)
4. A. Javidan, S. Rafizadeh, S.M. Hosseinpour-Mashkani, *Mater. Sci. Semicond. Process.* **27**, 468 (2014)
5. C.C. Homes, T. Vogt, S.M. Shapiro, S. Wakimoto, A.P. Ramirez, *Science* **293**, 673 (2001)
6. M.A. Subramanian, L. Dong, N. Duan, B.A. Reisner, A.W. Sleight, *J. Solid State Chem.* **151**, 323 (2000)
7. A.P. Ramirez, M.A. Subramanian, M. Gardel, G. Blumberg, D. Li, T. Vogt, S.M. Shapiro, *Solid State Commun.* **115**, 217 (2000)
8. M.C. Ferrarelli, T.B. Adams, A. Feteira, D.C. Sinclair, A.R. West, *Appl. Phys. Lett.* **89**, 212904 (2006)
9. C. Masingboon, S. Maensiri, T. Yamwong, P.L. Anderson, S. Seraphin, *Appl. Phys. A* **91**, 87 (2008)
10. M.A. Subramanian, D. Li, N. Duan, B.A. Reisner, A.W. Sleight, *J. Solid State Chem.* **151**, 323 (2000)
11. A.P. Ramirez, M.A. Subramanian, M. Gardel, G. Blumberg, D. Li, T. Vogt, S.M. Shapiro, *Solid State Commun.* **115**, 217 (2000)
12. C.C. Holmes, T. Vogt, S.M. Shapiro, S. Wakimoto, A.P. Ramirez, *Science* **293**, 637 (2001)
13. D.C. Sinclair, T.B. Adams, F.D. Morrison, A.R. West, *Appl. Phys. Lett.* **80**, 2153 (2002)
14. S.Y. Chung, I.L.D. Kim, S.J.L. Kang, *Nat. Mater.* **3**, 774 (2004)
15. R.K. Grubbs, E.L. Venturini, P.G. Clem, J.J. Richardson, B.A. Tuttle, G.A. Samara, *Phys. Rev. B* **72**, 104111 (2005)
16. T.T. Fang, H.K. Shiao, *J. Am. Ceram. Soc.* **87**, 2072 (2004)
17. T.B. Adams, D.C. Sinclair, A.R. West, *Adv. Mater. (Weinheim, Germany)* **14**, 1321 (2002)
18. J. Li, M.A. Subramanian, H.D. Rosenfeld, C.Y. Jones, B.H. Toby, A.W. Sleight, *Chem. Mater.* **16**, 5223 (2004)
19. S.M. Hosseinpour-Mashkani, M. Ramezani, M. Vatanparast, *Mater. Sci. Semicond. Process.* **26**, 112 (2014)
20. S.M. Hosseinpour-Mashkani, M. Ramezani, *Mater. Lett.* **130**, 259 (2014)
21. M. Zheng, R. Yu, J. Chen, J. Zhao, G. Liu, X. Xing, J. Meng, *J. Am. Ceram. Soc.* **91**, 544 (2008)